The AAV9 receptor and its modification to improve in vivo lung gene transfer in mice

Christie L. Bell,[1] Luk H. Vandenberghe,[1] Peter Bell,[1] Maria P. Limberis,[1] Guang-Ping Gao,[2] Kim Van Vliet,[3] Mavis Agbandje-McKenna,[3] and James M. Wilson[1]

[1]Gene Therapy Program, Department of Pathology and Laboratory Medicine, University of Pennsylvania, Philadelphia, Pennsylvania, USA. [2]Gene Therapy Center, University of Massachusetts Medical Center, Worcester, Massachusetts, USA. [3]Department of Biochemistry and Molecular Biology, University of Florida, Gainesville, Florida, USA.

Vectors based on adeno-associated virus (AAV) serotype 9 are candidates for in vivo gene delivery to many organs, but the receptor(s) mediating these tropisms have yet to be defined. We evaluated AAV9 uptake by glycans with terminal sialic acids (SAs), a common mode of cellular entry for viruses. We found, however, that AAV9 binding increased when terminal SA was enzymatically removed, suggesting that galactose, which is the most commonly observed penultimate monosaccharide to SA, may mediate AAV9 transduction. This was confirmed in mutant CHO Pro-5 cells deficient in the enzymes involved in glycoprotein biogenesis, as well as lectin interference studies. Binding of AAV9 to glycans with terminal galactose was demonstrated via glycan binding assays. Co-instillation of AAV9 vector with neuraminidase into mouse lung resulted in exposure of terminal galactose on the apical surface of conducting airway epithelial cells, as shown by lectin binding and increased transduction of these cells, demonstrating the possible utility of this vector in lung-directed gene transfer. Increasing the abundance of the receptor on target cells and improving vector efficacy may improve delivery of AAV vectors to their therapeutic targets.

Introduction

The first adeno-associated viral (AAV) vectors evaluated for gene therapy were based on serotype 2 (AAV2) and were shown to transduce a variety of somatic cells following in vivo delivery (1). One of the first clinical successes of gene therapy used an AAV2 vector to restore some aspects of vision following subretinal injection in patients with an inherited form of blindness (2, 3). Application of AAV2 vectors for the treatment of other diseases, however, has not been as successful due to poor transduction efficiencies and various immunologic problems such as preexisting neutralizing antibodies and T cell activation to the capsid (1). AAV2 is known to utilize heparan sulfate (HS) proteoglycans as a primary receptor for cellular recognition (2). Additional vectors were developed based on AAV capsids from other existing serotypes such as AAV1 and its close relative AAV6, both of which showed enhanced transduction of muscle and cellular binding mediated by sialylated glycoproteins (4, 5). Vectors based on AAV5 also require binding to N-linked sialic acid (SA) while showing enhanced transduction in CNS following direct injection in brain (6, 7).

The potential of AAV vectors for human gene therapy was expanded through the discovery of a large and diverse family of novel capsids from latent genomes in human and non-human primate tissues. This expanded family of AAVs numbers more than 120 genomes spanning 6 clades (8–10). High-resolution X-ray crystal structures and lower-resolution cryo-electron microscopy reconstructed images have been determined for many of the AAV capsids, demonstrating a highly conserved core region with a total of 9 surface-exposed hypervariable regions (11). Evaluation of vectors based on these novel endogenous capsids has been quite promising in terms of achieving substantially higher transduction efficiencies with diminished immunological sequelae (10). One of the more interesting vectors is based on AAV9 that was isolated from human DNA (9). AAV9 has shown significant promise in targeting the heart for treatment of cardiomyopathies (12) and neurons for treating diseases such as spinal muscular atrophy (13, 14). AAV9 also very efficiently transduces alveolar epithelial cells of the lung without eliciting a humoral response, allowing for efficient re-administration of vector (15).

The goal of our study was to identify key cellular receptor interactions with AAV9 and determine whether these could be modified to further improve its performance as a vector for human gene therapy.

Results

Initial attempts to identify cellular receptors that promote AAV9 transduction focused on a potential role of glycans with terminal SA. Previous studies have shown that α-2,3 and α-2,6 N-linked SA facilitates binding and transduction by AAV1 and -6 (4), while α-2,3 N-linked SA is important for transduction by AAV5 (6). Several previously described AAVs (serotypes 1, 2, 5, and 6) and the novel AAV serotypes 7, 8, 9, and -rh32.33 (8–10) were screened for binding to the CHO cell line Pro-5 with and without treatment with exo-α-sialidase from *Vibrio cholerae* (neuraminidase [NA]). This NA is capable of cleaving almost all known CHO, murine, and human SA linkages. Results with the first-generation AAVs were as expected, in that NA pretreatment (Figure 1A) had no effect on binding of AAV2, and binding of AAV1, AAV5, and AAV6 was diminished by at least 2 logs (Figure 1B). Studies with the novel AAVs failed to show an effect of NA treatment on binding of AAV7, -8, and -rh32.33, while AAV9 showed an unexpected 2.5-log increase in binding (Figure 1B). The impact of NA treatment on other cell lines commonly used in AAV studies, i.e., HEK293 (Figure 1C) and Huh-7

Conflict of interest: Luk H. Vandenberghe is an inventor on technologies described in this article that are licensed to various pharmaceutical and biotechnology companies. James M. Wilson is a consultant to ReGenX Holdings and is a founder of, holds equity in, and receives a grant from affiliates of ReGenX Holdings; in addition, he is an inventor on patents licensed to various biopharmaceutical companies, including affiliates of ReGenX Holdings.

Citation for this article: *J Clin Invest.* 2011;121(6):2427–2435. doi:10.1172/JCI57367.

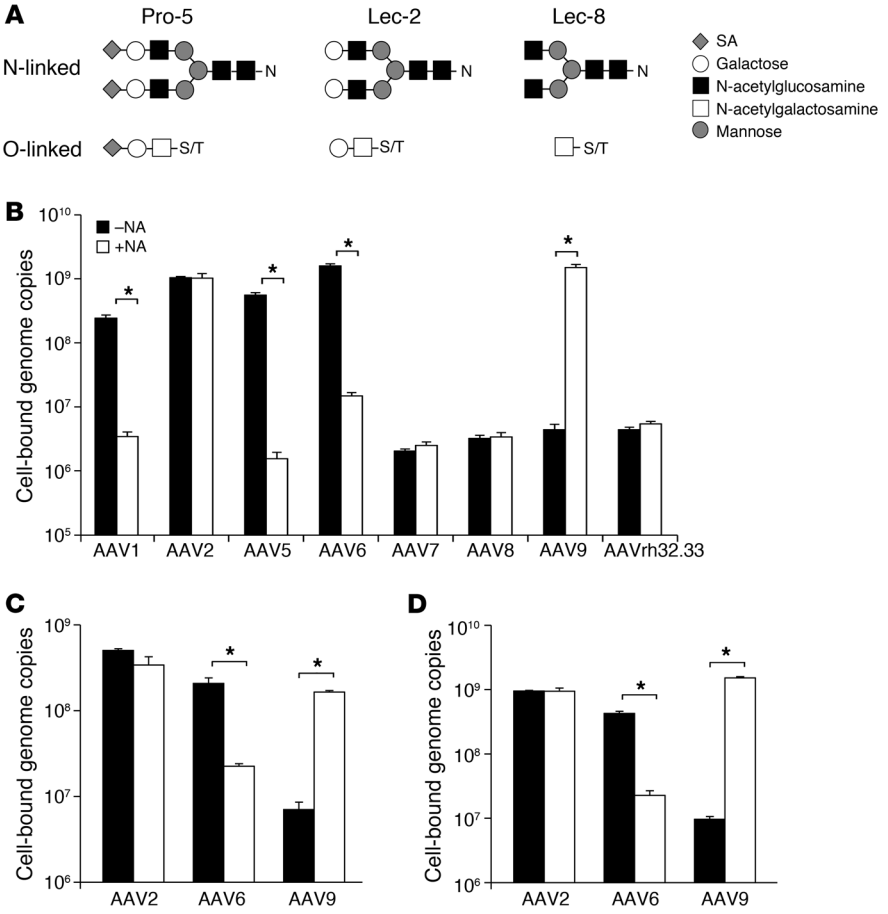

Figure 1
Effect of SA on AAV vector binding. (**A**) Schematic of N- and O-linked glycans for each CHO cell line (Pro-5, Lec-2, and Lec-8; ref. 17). Pretreating Pro-5 cells with NA alone or NA and β-gal should produce glycan structures similar to those seen in Lec-2 and Lec-8 cells, respectively. (**B**–**D**) SA was removed from the surface of (**B**) Pro-5, (**C**) HEK293, and (**D**) Huh-7 cells by treatment with NA from *Vibrio cholerae*. AAV vectors (5×10^9 genome copies; MOI, 10^4) were applied to NA-treated and untreated cells and incubated at 4°C for 1 hour. After extensive washing, total DNA was isolated and bound vector was quantified by qPCR. $^*P < 0.001$.

(Figure 1D), was evaluated. For both cell lines, NA had no effect on AAV2 binding, while it decreased binding of AAV6 and increased binding of AAV9 to the same extent as observed with Pro-5 cells. The electrophoretic mobility of the 3 primary capsid proteins of AAV9 — VP1, VP2, and VP3 — was unaffected when purified vector was treated with various glycosidases (Supplemental Figure 1; supplemental material available online with this article; doi:10.1172/JCI57367DS1). This suggests that the capsid is not glycosylated, which is consistent with studies of other AAV serotypes (16) and supports the hypothesis that the NA-mediated effect is due to modification of a cellular receptor, not the capsid.

We speculated that the presence of terminal SA on an oligosaccharide of a receptor either inhibited binding to AAV9 or that the removal of SA exposed a molecule that enhanced binding. The most likely candidate would be β-1,3 or β-1,4 galactose, which is the penultimate monosaccharide on most SA-rich glycans (Figure 1A). These hypotheses were initially explored using somatic cell mutants of the parent CHO cell line, Pro-5, which are deficient in various enzymes involved with glycosylation by virtue of lectin resistance (17). Lec-2 is deficient in cytidine monophosphate–SA (CMP-SA) Golgi transporter and should have a full complement of N- and O-glycans that are missing terminal SA (Figure 1A). Lec-8 is deficient in uridine diphosphate galactose (UDP-galactose) Golgi transporter and should produce N- and O-glycans that are missing both SA and galactose saccharides (Figure 1A). Vectors based on AAV2, -6, and -9 expressing firefly luciferase (ffLuc) were incubated with Pro-5, Lec-2, and Lec-8 cells and analyzed for binding and transduction (Figure 2, A and B). Binding and transduction of AAV2 was the same in all 3 cell lines and decreased with AAV6 in Lec-2 and Lec-8 cells relative to Pro-5 cells, which was expected based on previous studies demonstrating the importance of SA in facilitating AAV6 entry (4). For AAV9, binding and transduction increased substantially in Lec-2 but decreased to baseline levels in Lec-8 cells, which is more consistent with the hypothesis that binding to terminal β-galactose facilitates uptake, rather than that SA inhibits uptake. The concurrence of binding with transduction suggests that binding to terminal galactose is an important step in AAV9 transduction. The impact of eliminating SA was greater on binding than on transduction, suggesting that post-entry steps may also limit transduction.

The role of terminal galactose in AAV9 binding was further studied in Pro-5 cells that were pretreated with NA and then cocultured with lectins of different specificities (Figure 2C, binding; Figure 2D, transduction). The only lectins that blocked binding of AAV9 were *Erythrina cristagalli* lectin (ECL), which recognizes β-1,4 galactose, and *Ricinus communis* agglutinin I (RCA I), which recognizes several types of β-galactose linkages, with β-1,4 galactose showing the highest affinity; neither affected binding of AAV2. Lectins that recognize α-galactose (*Griffonia simplicifolia* lectin I isolectin B_4 [GSL B_4]), α-1,3 and α-1,6 mannose (*Hippeastrum* hybrid lectin [HHL]), and α-fucose (*Lotus tetragonolobus* lectin [LTL]) did not interfere with binding of AAV2 or AAV9. Wheat germ agglutinin (WGA) had a slight effect on AAV9 binding, likely due to its interaction with *N*-acetylglucosamine, which is commonly bound to

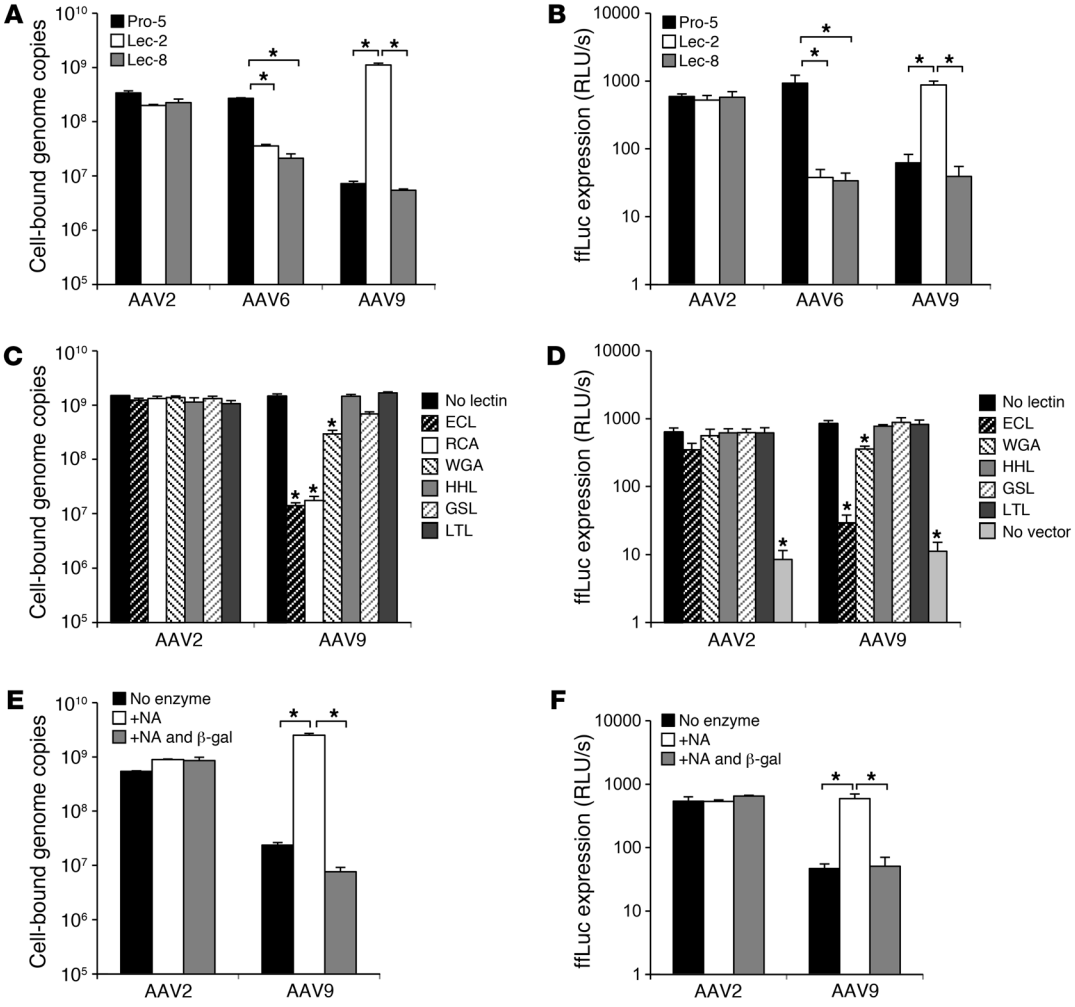

Figure 2

AAV9 dependence on galactose for binding and transduction of CHO cells. (**A** and **B**) AAV2, AAV6, or AAV9 expressing ffLuc was added to Pro-5, Lec-2, or Lec-8 cells and incubated at 4°C for 1 hour. (**A**) Total DNA was isolated to determine bound vector genome copies by qPCR or (**B**) cells were incubated at 37°C for 48 hours and analyzed for ffLuc expression. (**C** and **D**) AAV2 and AAV9 were applied to NA-treated Pro-5 cells in the presence of various lectins to compete for AAV binding (**C**) or transduction (**D**). RCA was not used in transduction studies because of its toxicity to the cells. (**E** and **F**) AAV2 and AAV9 were added to Pro-5 cells that were treated with either NA or both NA and β-gal to assess AAV binding (**E**) and transduction (**F**). *$P < 0.001$. For **C** and **D**, statistical significance was determined compared with the no lectin control.

galactose. Lectin inhibition of AAV2 and AAV9 transduction confirmed the binding results, except in the case of RCA, which was not informative since it was toxic to cells.

A final confirmation of the glycan specificity of AAV9 uptake was performed in Pro-5 cells pretreated with NA to cleave terminal SA or a combination of NA and β-gal that would remove both NA and β-galactose saccharides (Figure 1A). Binding and transduction with AAV2 was unaffected by enzyme pretreatment, while NA enhanced transduction of AAV9 as described earlier, an effect that was reversed by subsequent treatment with β-gal (Figure 2, E and F).

The glycan-capsid interactions of AAV9 were further interrogated using a glycan microarray (GMA) composed of 465 different natural and synthetic mammalian glycans that contains 6 replicates for each glycan. A similar strategy was used to verify the binding of AAV1 to sialylated glycans as determined by biochemical and molecular approaches (4). In our analysis, each glycan was evaluated for binding as measured by relative fluorescence units (RFU) in terms of the mean of 4 replicates within the array ± 1 SD (the highest and lowest binding within the 6 replicates were eliminated). Variation within the 4 replicates was assessed as the coefficient of variation (%CV), which was considered low if it was less than 20. The selection of glycans with specific binding affinity for AAV9 capsids was based on two independent criteria: high overall total binding as measured by RFU and low variation among the 4 replicates as assessed by %CV. The highest binding glycans were arbitrarily defined as those with mean RFU values that fell within 3 SD of the highest binding glycan, 415. Of the 4 glycans that fulfilled the criteria of high binding affinity, 3 showed high specificity as indicated by a %CV less than 20 (Figure 3). These 3 glycans, 415, 297, and 399, demonstrated sufficient affinity and specificity to be considered potential receptors for AAV9 binding. The 3 glycans selected as being specific for binding to AAV9 based

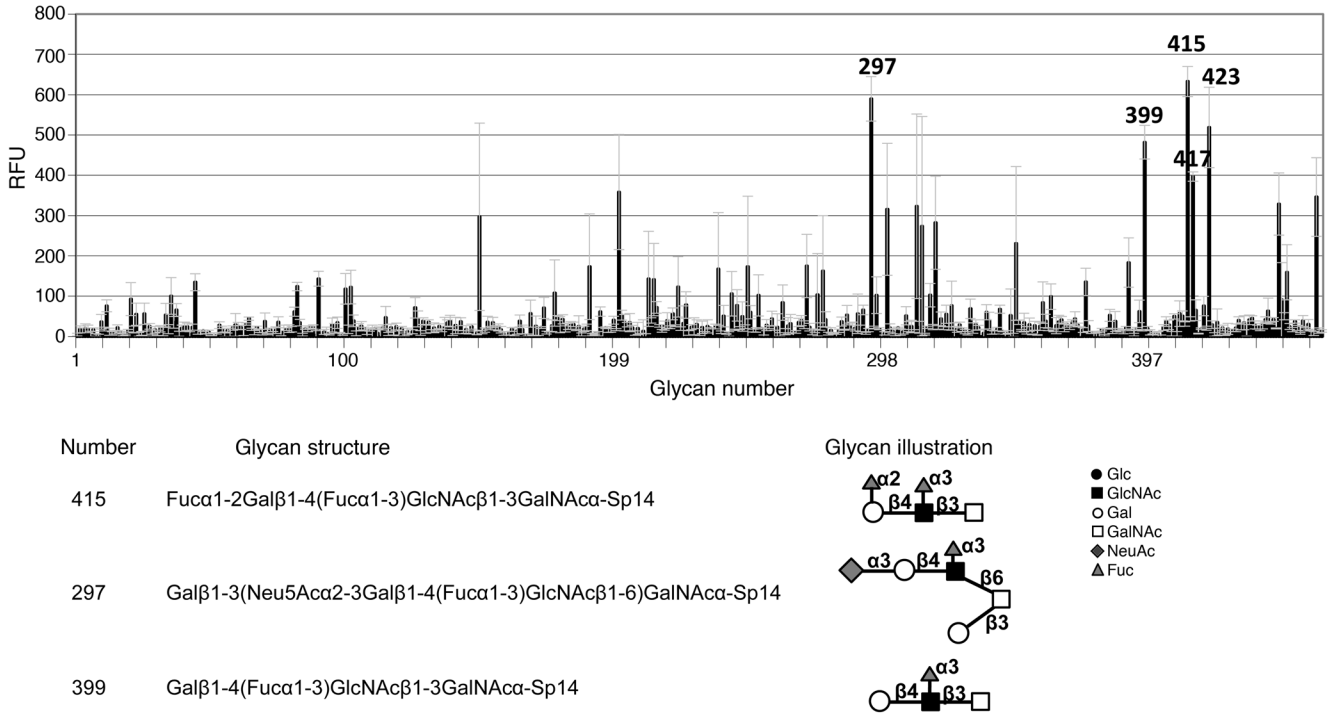

Figure 3
GMA analysis of AAV9 binding. AAV9 capsids were screened for binding to 465 different glycans based on the average relative fluorescence, with the top 5 glycans that bound AAV9 indicated (number indicates glycan identifier). Error bars represent the SD of glycan binding. The structures of the top 3 glycans with high specificity of binding and their representative illustrations are shown in the bottom panel. The average RFU and %CV for each glycan were as follows (glycan identifier: average RFU, %CV): 415: 633, 12; 297: 590, 19; and 399: 482, 17.

on total binding and specificity of binding were all shown to have terminal galactose (Gal) with either β-1,4 linkages (i.e., 415 and 399) or a β-1,3 linkage (297, Figure 3). Each glycan contains Galβ1-4(Fucα1-3)GlcNAc linked via β1-3 or β1-6 to GalNAc in its structure, suggesting a structural context of the SA-deficient glycan for binding to AAV9. Reconciling the binding data with cell-based binding/transduction experiments confirmed the role of terminal β-galactose linkages in tropism of AAV9.

The relevance of the novel β-galactose–mediated uptake pathway for AAV9 to in vivo gene delivery was evaluated in the context of lung-directed gene transfer. Previously we showed that delivery of AAV9 vectors into lungs of mice resulted in efficient transduction of epithelial cells of the alveoli but no transduction of epithelial cells of the conducting airway, which is the preferred target for the treatment of cystic fibrosis (15). Studies were performed in mice to determine whether transduction of conducting airway with AAV9 could be enhanced by pretreating mouse airways with a formulation that contained NA. Comparisons were made to mice administered AAV6, which in previous studies showed efficient in vivo transduction of conducting airway (18). Based on in vitro studies with cell lines, this in vivo transduction may be dependent on binding to SA (4). Figure 4, A–D, shows representative histochemical analyses of lung tissue, while Figure 4E presents a morphometric analysis of *lacZ*-positive cells in conducting airway. Lung delivery of AAV9 in the absence of NA demonstrated the expected pattern of alveolar-restricted transduction (Figure 4, A, B, and E). Administration of NA into the lung 1 hour prior to or at the time of AAV9 administration yielded a very different pattern, with high-level transduction in both the alveolar and conducting airway epithelial cells (Figure 4, A, B, and E). The high-level transduction of conducting airway obtained with AAV6 was completely eliminated when animals were treated with NA, confirming the dependence of in vivo transduction on binding to SA (Figure 4, C–E). The consequences of airway delivery of NA on the abundance and distribution of glycan structure were studied directly by staining lung sections with fluorescence-labeled lectins that bind terminal galactose residues with β linkages (RCA) or terminal SA residues (SNA). Prior to NA treatment, staining with RCA was limited to alveolar cells and the basolateral region of conducting airways (Figure 5, A and C). A similar pattern was observed with SNA, although the apical surface of the conducting airway was also stained (Figure 5, B and D). Treatment with NA had the most dramatic effect on the staining of conducting airway epithelial cells, which was substantially increased with respect to RCA (Figure 5, E and G) and moderately reduced with respect to SA (Figure 5, F and H). Higher-resolution microscopic studies were performed to determine whether RCA binding localized to the plasma membrane or the overlying mucus layer. Lung sections from animals pretreated with NA were evaluated for colocalization of RCA staining with immune localization of α-tubulin, which delineates the cilia from the apical surface of airway epithelial cells (Figure 5, I–K). These studies demonstrated binding of RCA to the cell surface of epithelial cells in the conducting airway of NA-pretreated lungs.

A major impediment to transduction following intravascular (IV) administration of AAV vectors is the physical barrier of the contiguous endothelium and basal lamina of the microcirculation. The

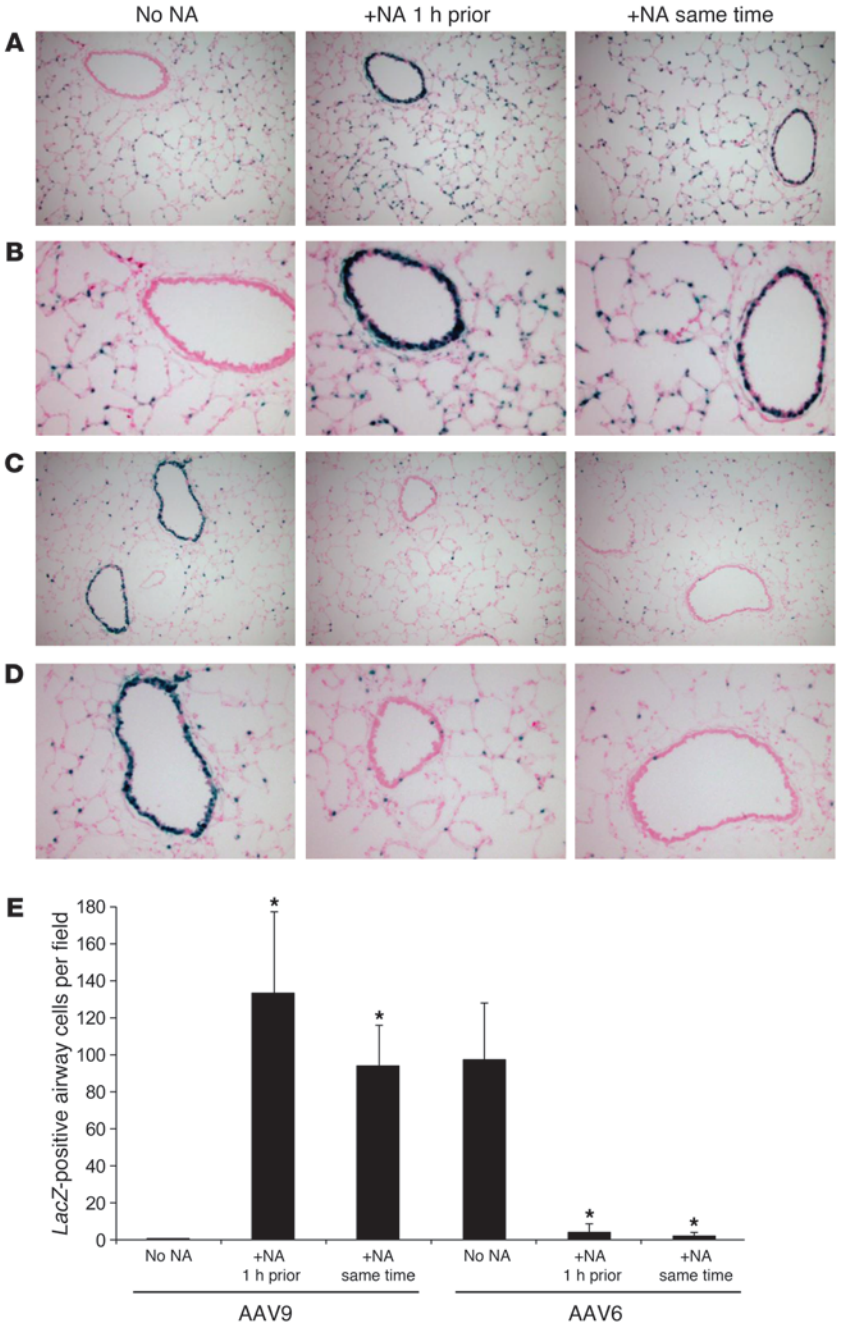

Figure 4
AAV9 transduction of murine conducting airway following pretreatment with NA. C57BL/6 mice were given an intranasal instillation of 10^{11} genome copies of AAV9 (**A** and **B**) or AAV6 expressing n*LacZ* (**C** and **D**) either 1 hour after intranasal instillation of 100 mU NA or simultaneously with the NA treatment. AAV9 vector administered without NA was used as a control. At day 21 after administration, lungs were harvested and sections stained for β-gal expression. Lung sections were examined at both ×100 magnification (**A** and **C**) and ×200 magnification (**B** and **D**) for each condition. (**E**) n*LacZ*-positive cells in the conducting airway were quantified for each group as the average number of n*LacZ*-positive cells ± SD per ×200 field of view. **P* < 0.001 compared with the no NA control.

one exception is the liver, which contains fenestrated endothelia, allowing direct access of vector in blood to the hepatocytes. AAV9 is unique in that it partially overcomes this barrier, allowing targeting of skeletal and cardiac muscle and, to a lesser extent, cells of the central nervous system (13, 14, 19). We analyzed *lacZ* transduction following IV administration of AAV9 vector at doses of 10^{11} and 10^{12} genome copies (GC)/mouse (Figure 6, A–C). This was correlated with the presence of terminal β-galactose through staining with RCA (Figure 6, A–C). As has been described, liver was efficiently transduced even at low doses of vector (Figure 6C and ref. 20); it was possible to efficiently transduce cardiac and skeletal muscle at higher vector doses (Figure 6, A and B, and ref. 19). Surfaces of muscle fibers from skeletal and cardiac tissues demonstrated high levels of terminal β-galactose, as evidenced by binding to RCA (Figure 6, A and B). Hepatocytes demonstrated lower levels of RCA binding, although endothelial surfaces of hepatic vessels stained brightly (Figure 6C).

Several AAVs such as AAV5 and AAVrh.10 are capable of efficient transduction of cells of the CNS following direct injection, although transduction is limited to regions in proximity to the needle injection site (7, 21). AAV9 has demonstrated the unique properties of detectable transduction of the CNS following intravenous injection (13, 14). We evaluated brain for the presence of β-galactose terminal glycans via binding to RCA, which showed high levels in small vessels as demonstrated by colocalization with the endothelial-specific marker CD31 (Figure 6D).

Discussion

Understanding the biology of AAV9 transduction is important in light of its potential clinical utility and unique properties. Vectors based on this human-derived virus show an extraordinarily wide biodistribution when administered directly to animals (13, 14, 19). AAV9 vectors have the ability to traverse the physical barrier of endothelia of the vascular system following IV injection, which has been used to target heart for treatment of heart failure, skeletal muscle for treatment of muscular dystrophy, and neurons for treatment of a variety of neuromuscular disorders (13, 14, 19, 20). Furthermore, AAV9 elicits very little neutralizing antibody responses, thereby allowing its successful re-administration into the lung (15).

We focused on the potential role of glycans in mediating AAV9 transduction since they often serve as receptors for virus infection, usually with exquisite specificity with respect to the component monosaccharide. Specific interactions with glycans containing terminal SA have been described for many viruses including several other AAV serotypes. Our finding that binding and transduction by AAV9 occurs via terminal β-galactose linkages has not been described for any other virus including the known AAVs, although norovirus binds to glycans with α-galactose linkages (22).

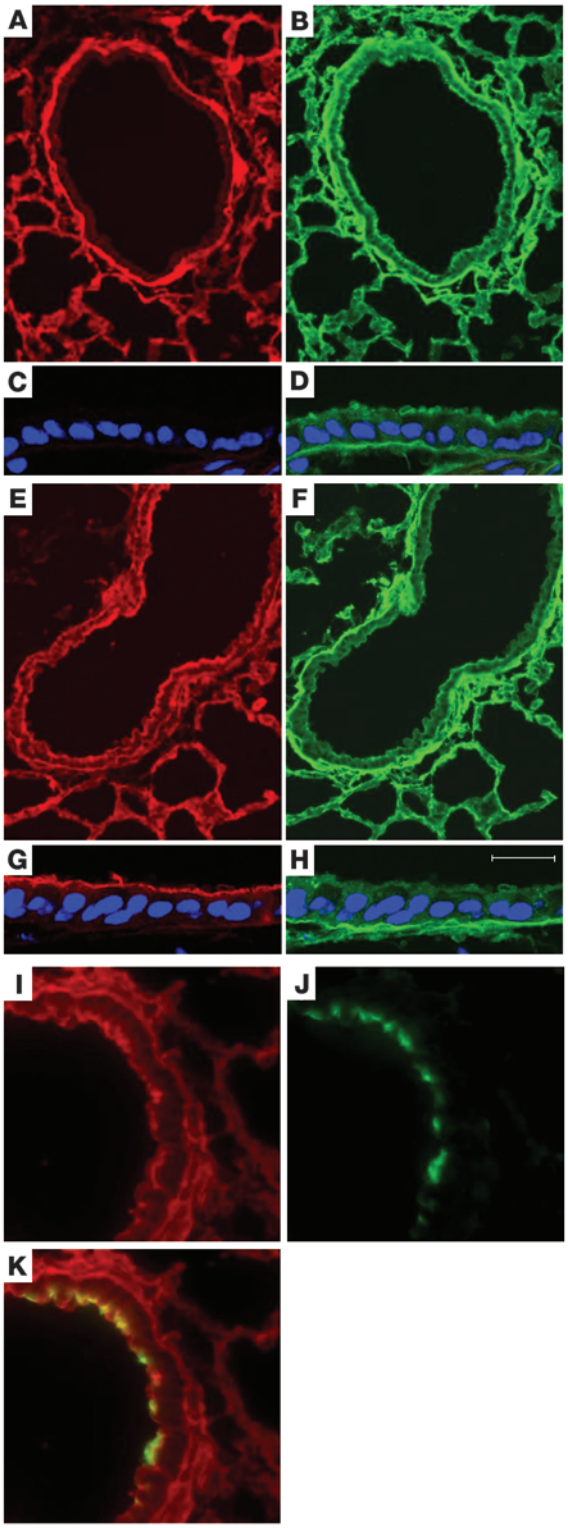

Figure 5
Expression of galactose in the cells of the murine conducting airways. C57BL/6 mice were treated with PBS (**A**–**D**) or 100 mU NA (**E**–**H**) in a total of 30 μl delivered intranasally. Lungs were inflated and removed 1 hour later, and thin sections (8 μm) were stained with (**A**, **C**, **E**, and **G**) rhodamine-RCA, (**B**, **D**, **F**, and **H**) fluorescein-SNA, and (**C**, **D**, **G**, and **H**) DAPI. Sections were examined by wide-field ×200 magnification (**A**, **B**, **E**, and **F**) and confocal microscopy (**C**, **D**, **G**, and **H**). Scale bar: 20 μm. (**I**–**K**) Lung sections of mice treated intranasally with NA were stained for (**I**) galactose expression using rhodamine–RCA lectin and (**J**) α-tubulin expression to stain cilia. (**K**) Overlay of galactose and α-tubulin staining. Sections were examined at ×400 magnification.

Glycan array studies demonstrated specific binding of AAV9 to 3 glycans, all of which contained terminal β-galactose linkages, confirming the importance of this saccharide in transduction, as was delineated in multiple cell lines using 3 independent approaches (i.e., glycosidase pretreatment, lectin competition, and somatic cell mutants). These glycans all contained Galβ1-4(Fucα1-3)GlcNAc linked via β1-3 or β1-6 to GalNAc in their structures and were linked via threonine through a GalNAc, indicating that *O*-linked galactose-containing glycans are capable of binding to AAV9, although functional interactions with glycans associated with other types of linkages cannot be ruled out (23). An important caveat regarding the binding data is that binding affinity does not necessarily correlate with functional significance in terms of glycosylated receptors that mediate transduction.

The receptors for important gene therapy vectors have been well characterized in vitro, but rarely has the significance of these receptors for in vivo transduction been confirmed. One example of a discordance between in vitro and in vivo transduction is that of human adenovirus 5 (Ad5). The coxsackievirus and adenovirus receptor (CAR) was isolated as the receptor for Ad5 based on in vitro studies (24, 25) and attempts to confirm the importance of CAR following in vivo gene transfer utilized CAR binding–ablated Ad5 (26–28). Following intravenous administration, the transduction levels and the liver-selective profile of CAR binding–ablated Ad5 vectors were similar to those of Ad5, suggesting potential redundant uptake pathways in vivo. Investigation of the mechanism of Ad5 transduction in vivo revealed that the presence of blood coagulation factors could mediate transduction through a non-CAR-dependent pathway (29–31). In comparison, our studies with AAV9 vectors following lung-directed gene transfer in combination with NA provided direct confirmation of the importance of β-galactose linkages in transduction of conducting airway epithelial cells by AAV9.

Evaluating the role of β-galactose linkages in transducing cells of tissues other than the lungs following in vivo gene transfer is more complicated due to barriers of delivery that are not present when vector is delivered into the airway allowing direct access to epithelial cells. Transduction following IV administration of AAV9, which is a route of administration being considered in many clinical applications of gene therapy, illustrates this point. IV infusion of vectors based on most AAV serotypes results in transduction primarily limited to hepatocytes because the fenestrae of the hepatic sinusoids eliminate the vascular barrier (32). In our studies, AAV9 efficiently transduced hepatocytes despite limited levels of β-galactose. Higher doses of AAV9 can overcome the vascular barrier and efficiently transduce cardiac and skeletal muscle fibers that do contain high levels of cell surface β-galactose glycans. As noted by several groups, AAV9 uniquely traverses the even more fortified blood brain barrier to allow limited transduction of neurons (13, 14). We speculate that the presence of glycans with β-galactose linkages on the surface of endothelial cells of some vascular structure, as we have shown in the brain, may be involved in facilitating this egress, possibly through a process of transcytosis.

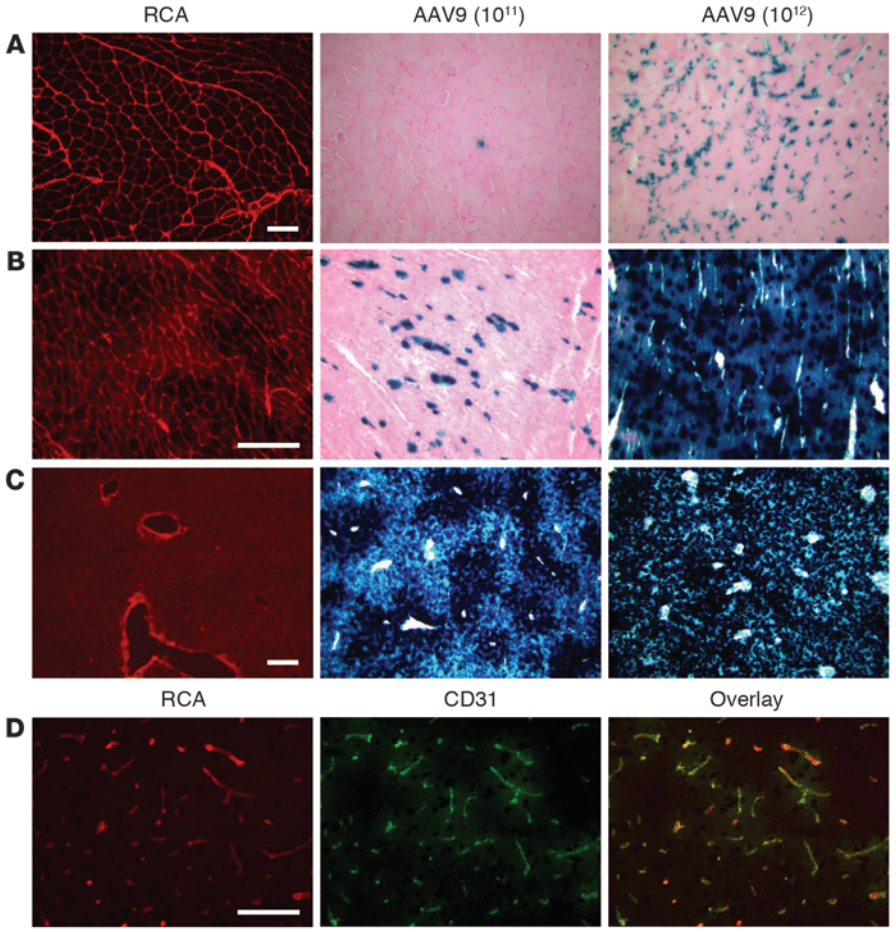

Figure 6
Correlation of galactose expression and AAV vector transduction in mouse organs. (**A**–**C**) Comparison of RCA staining of (**A**) muscle, (**B**) heart, and (**C**) liver with AAV vector transduction efficiency after IV injection of AAV9.CB.n*LacZ* at 2 different doses (10^{11} and 10^{12} GC) at day 21. (**D**) RCA staining of capillaries in brain and costaining with an antibody against CD31 as an endothelial marker. Scale bars: 100 μm.

The demonstrated binding of AAV9 to O-linked glycans of diverse structures suggests that interactions with non-cell-mediated glycoproteins such as in blood or in mucosal surfaces may modulate biodistribution of vector and transduction profiles.

Identification of the primary receptor for AAV9 was also useful in developing a pharmacologic approach for enhancing its transduction in conducting airway of the lung. This concept may be helpful in other in vitro and in vivo applications of gene transfer where the receptor is known. The key will be a safe and efficient method of modifying the receptor to improve transduction, which was simply done with AAV9 for the lung by formulating AAV9 with a carrier that included NA. It will be interesting to determine whether such an effect can be achieved for other targets of AAV9, particularly when the NA-formulated vector can be administered directly into tissue such as the retina or into a closed space such as a joint.

During the review of this article, Shen et al. published a report confirming the importance of glycans with terminal β-galactose linkages in mediating transduction of AAV9 in vitro and in nasal mucosa (33). Using glycosylation inhibitors, they implicated an N-linked glycan in AAV9 transduction.

Methods

Vector production and purification. AAV vectors were produced as previously described by the Penn Vector Core (http://www.med.upenn.edu/gtp/vector_core/production.shtml). Briefly, a plasmid encoding the transgene of interest, ffLuc, expressed from a cytomegalovirus promoter or nuclear-targeted *LacZ* (n*LacZ*) expressed from a chicken β-actin promoter, flanked by AAV2 inverted terminal repeats, was packaged by triple transfection of HEK293 cells with plasmids encoding the AAV2 *rep* gene and the AAV1, -2, -5, -6, -7, -8, -9, or rh32.33 *cap* gene and an adenovirus helper plasmid (pAdΔF6). Vectors were purified by cesium chloride gradient centrifugation and titers determined by quantitative PCR (qPCR).

Cell lines. Three different CHO cell lines were used in AAV binding and transduction studies. These were obtained from ATCC and include the parental cell line Pro-5, the SA-deficient cell line Lec-2, and the galactose-deficient cell line Lec-8. These cells were cultured in α–minimum essential medium (α-MEM) supplemented with ribonucleosides and deoxyribonucleosides (Invitrogen) with 10% FBS and 1% penicillin/streptomycin. HEK293 and Huh-7 cells were cultured in DMEM with 10% FBS and 1% penicillin/streptomycin.

Animals. Male C57BL/6 mice (6–8 weeks) were purchased from The Jackson Laboratory and maintained in the pathogen-free Animal Facility of the Translational Research Laboratories at the University of Pennsylvania. All animal procedures were approved by the Institutional Animal Care and Use Committee of the University of Pennsylvania.

Cell binding and transduction assays. For binding assays, cells were scraped from 150-cm^2 flasks and seeded onto 96-well plates at 5×10^5 cells/well in 100 μl cold serum-free (SF) medium. AAV vectors were added at 5×10^9 GC/well in 100 μl cold SF medium and incubated at 4°C for 1 hour. Cells were then washed 3 times with SF medium and resuspended in 200 μl PBS. Total DNA was extracted using the QIAamp DNA Mini Kit (QIAGEN). Cell-bound genome copies were quantified by real-time PCR. Primers and probe used were complementary to the SV40 polyA sequence of the vector genome: F primer, AGCAATAGCATCACAAATTTCACAA; R primer, CCAGACATGATAAGATACATTGATGAGTT; TaqMan probe, 6FAM-AGCATTTTTTTCACTGCATTCTAGTTGTGGTTTGTC-TAMRA. For cell transduction assays, cells were seeded at 10^5 cells/well in black-walled, clear-bottom 96-well plates overnight. Plates were then placed at 4°C for 15 minutes, and 10^9 GC of AAV vector expressing ffLuc was added in 100 μl cold SF medium and incubated for 1 hour at 4°C. Cells were then washed 3 times with SF medium. Warm medium containing serum was supplemented, and cells were incubated at 37°C for 48 hours. ffLuc expression was monitored by adding 150 μg/ml D-luciferin substrate per well and measuring the relative light units/second (RLU/s) using a luminometer.

Glycosidase treatment and lectin competition. Pro-5 cells were treated with 50 mU/ml NA type III from *Vibrio cholerae* (Sigma-Aldrich) in 100 μl SF medi-

um or control cells with medium alone for 2 hours at 37 °C. Some cells were then additionally treated with 60 mU/ml β-(1→4)-galactosidase in 50 μl reaction buffer (Sigma-Aldrich) or control cells with reaction buffer alone for 3 hours at 37°C. Cells were then washed 3 times before the binding and transduction studies, as described above. For lectin competition studies, Pro-5 cells were first treated with NA to remove SA. Cells were washed with cold SF medium, and lectins were added at 50 μg/ml in 100 μl SF medium or medium alone as control and incubated at 4°C for 15 minutes. The lectin solution was then removed, and a mixture of AAV vector (5×10^9 GC for binding assays and 10^9 GC for transduction assays) and 50 μg/ml lectin or vector alone as control was added and incubated at 4°C for 1 hour. Cells were then washed and analyzed for AAV binding or transduction as described above. Lectins used in this study include ECL, which binds galactosyl (β-1,4) N-acetylglucosamine; RCA I, which binds terminal galactose residues; WGA, which binds N-acetylglucosamine and also interacts via SA; HHL, which binds α-1,3 and α-1,6 mannose; GSL B_4, which binds α-galactose; and LTL, which binds α-linked fucose (Vector Laboratories).

Screening of glycan binding specificity of AAV9. The baculovirus/Sf9 protein expression system provides a tractable method for the production of large quantities of AAV virus-like particles (VLPs) shown to be structurally and antigenically similar to virus particles and virions produced in mammalian cell culture systems (34, 35). For GMA binding studies, VLPs of AAV9 were prepared using the Bac-to-Bac baculovirus/Sf9 expression system (Invitrogen) as previously described (36) and screened in a high-throughput GMA developed by Cores D and H of the Consortium for Functional Glycomics (CFG; an NIH National Institute of General Medicine Science Initiative; ref. 37). The printed array (V4.1, http://www.functionalglycomics.org/static/consortium/resources/resourcecoreh14.shtml) was composed of 465 different natural and synthetic mammalian glycans, including sialylated sugars with different linkages and modifications, and was generated using amine coupling to covalently link amine-functionalized glycans or glycan conjugates to an amine-reactive N-hydroxysuccinimide–activated glass slide. A printed slide, containing 6 replicates per glycan or glycoconjugate, was incubated with AAV9 VLPs at 200 μg/ml, then ADK9, a capsid monoclonal antibody (provided by Jürgen Kleinschmidt, Applied Tumor Virology, German Cancer Research Centre, Heidelberg, Germany) was overlaid on the bound capsids, followed by a FITC-labeled secondary antibody (at 5 μg/ml) for detection. Fluorescence intensity was detected using a ScanArray 5000 confocal scanner (PerkinElmer). IMAGENE image analysis software (BioDiscovery) was used to analyze the image. The relative binding for each glycan was expressed as mean RFU of 4 of the 6 replicates, calculated without using the highest and lowest values. The binding data were analyzed using two selection criterion: (a) glycans that were within 3 SDs of the mean of the glycan with the highest RFU value; and (b) glycans with %CV of less than 20% between the RFUs of the 4 replicates used to calculate the average RFU value (with %CV defined as the ratio of the SD of the data to the mean expressed as a percentage). Information relevant to the generation of the glycan array data are available at http://www.functionalglycomics.org/glycomics/HServlet?operation=view&sideMenu=no&psId=primscreen_3528. Included in this data set are the raw data, the normalized data, sample annotation, experimental design, annotation of the glycan array, and experimental protocols (accession id primscreen_3528).

In vivo NA experiments. Mice were anesthetized with ketamine/xylazine and given intranasal instillation of 10^{11} GC of AAV with or without 100 mU NA in 50 μl PBS. NA was administered either 1 hour prior to or simultaneously with vector instillation. n*LacZ* gene expression in the lungs was examined 21 days after administration by methods previously described (38). Lung sections were examined at both ×100 and ×200 magnification. *LacZ*-positive cells in the conducting airways were quantified by counting positive cells per ×200-magnification field of view.

Lectin staining. Mice were anesthetized with ketamine/xylazine and given an intranasal instillation of 100 mU NA in 30 μl PBS or PBS alone as control. Lungs were harvested 1 hour later by methods previously described (38) and sections fixed in cold (–20°C) acetone for 5 minutes. The lung sections were then blocked with Carbo-Free Blocking Solution (Vector Laboratories) and incubated with 15 μg/ml rhodamine-labeled RCA I and 7.5 μg/ml fluorescein-labeled *Sambucus nigra* lectin (SNA) for 30 minutes at room temperature. Slides were then washed twice in PBS and mounted in Vectashield with DAPI (Vector Laboratories). Images were taken by both wide-field (×200) and confocal microscopy (Zeiss LSM 510 confocal microscope). For RCA staining of muscle, heart, liver, and brain, organs were removed from untreated mice and sections stained as above. For CD31 staining of brain, slides were incubated with rat anti-CD31 primary antibody (BD Biosciences — Pharmingen), followed by fluorescein-labeled anti-rat secondary antibody (Vector Laboratories) and rhodamine-labeled RCA. For α-tubulin staining of lung, slides were processed as above, except sections were fixed in 4% paraformaldehyde and stained with mouse anti–α-tubulin primary antibody (Sigma-Aldrich), followed by fluorescein-labeled horse anti-mouse secondary antibody (Vector Laboratories) and rhodamine-labeled RCA. Images were taken at ×400 magnification.

Statistics. Statistical significance was determined using Student's 2-tailed *t* test. *P* values of less than 0.001 were considered significant. Data are represented as mean ± SD.

Acknowledgments

We thank Jürgen Kleinschmidt for providing antibody ADK9 for these studies. The glycan array analysis was conducted by the Consortium for Functional Glycomics, Protein-Carbohydrate Interaction Core H, funded by National Institute of General Medical Sciences grant GM62116. This project was funded in part by NIH R01 GM082946 (to M. Agbandje-McKenna), NIH P01 HL059407 (to J.M. Wilson), NIH P30 DK047757 (to J.M. Wilson), NIH T32 DK007748 (to C.L. Bell), and a sponsored research agreement from ReGenX (to J.M. Wilson).

Received for publication February 1, 2011, and accepted in revised form April 7, 2011.

Address correspondence to: James M. Wilson, Gene Therapy Program, Department of Pathology and Laboratory Medicine, University of Pennsylvania, 125 S. 31st Street, Suite 2000 TRL, Philadelphia, Pennsylvania 19104, USA. Phone: 215.898.0226; Fax: 215.898.6588; E-mail: wilsonjm@mail.med.upenn.edu.

Luk H. Vandenberghe's present address is: F.M. Kirby Center for Molecular Ophthalmology, University of Pennsylvania, Philadelphia, Pennsylvania, USA.

1. Wu Z, Asokan A, Samulski RJ. Adeno-associated virus serotypes: vector toolkit for human gene therapy. *Mol Ther*. 2006;14(3):316–327.
2. Kern A, et al. Identification of a heparin-binding motif on adeno-associated virus type 2 capsids. *J Virol*. 2003;77(20):11072–11081.
3. Maguire AM, et al. Safety and efficacy of gene transfer for Leber's congenital amaurosis. *N Engl J Med*. 2008;358(21):2240–2248.
4. Wu Z, Miller E, Agbandje-McKenna M, Samulski RJ. Alpha2,3 and alpha2,6 N-linked sialic acids facilitate efficient binding and transduction by adeno-associated virus types 1 and 6. *J Virol*. 2006; 80(18):9093–9103.
5. Xiao W, Chirmule N, Berta SC, McCullough B, Gao G, Wilson JM. Gene therapy vectors based on adeno-associated virus type 1. *J Virol*. 1999;73(5):3994–4003.
6. Walters RW, et al. Binding of adeno-associated virus

type 5 to 2,3-linked sialic acid is required for gene transfer. *J Biol Chem*. 2001;276(23):20610–20616.
7. Davidson BL, et al. Recombinant adeno-associated virus type 2, 4, and 5 vectors: transduction of variant cell types and regions in the mammalian central nervous system. *Proc Natl Acad Sci U S A*. 2000; 97(7):3428–3432.
8. Gao G, et al. Adeno-associated viruses undergo substantial evolution in primates during natural infections. *Proc Natl Acad Sci U S A*. 2003; 100(10):6081–6086.
9. Gao G, et al. Clades of Adeno-associated viruses are widely disseminated in human tissues. *J Virol*. 2004; 78(12):6381–6388.
10. Gao GP, Alvira MR, Wang L, Calcedo R, Johnston J, Wilson JM. Novel adeno-associated viruses from rhesus monkeys as vectors for human gene therapy. *Proc Natl Acad Sci U S A*. 2002;99(18):11854–11859.
11. Nam HJ, et al. Structure of adeno-associated virus serotype 8, a gene therapy vector. *J Virol*. 2007; 81(22):12260–12271.
12. Bish LT, et al. Adeno-associated virus (AAV) serotype 9 provides global cardiac gene transfer superior to AAV1, AAV6, AAV7, and AAV8 in the mouse and rat. *Hum Gene Ther*. 2008;19(12):1359–1368.
13. Duque S, et al. Intravenous administration of self-complementary AAV9 enables transgene delivery to adult motor neurons. *Mol Ther*. 2009; 17(7):1187–1196.
14. Foust KD, Nurre E, Montgomery CL, Hernandez A, Chan CM, Kaspar BK. Intravascular AAV9 preferentially targets neonatal neurons and adult astrocytes. *Nat Biotechnol*. 2009;27(1):59–65.
15. Limberis MP, Wilson JM. Adeno-associated virus serotype 9 vectors transduce murine alveolar and nasal epithelia and can be readministered. *Proc Natl Acad Sci U S A*. 2006;103(35):12993–12998.
16. Murray S, et al. Characterization of the capsid protein glycosylation of adeno-associated virus type 2 by high-resolution mass spectrometry. *J Virol*. 2006; 80(12):6171–6176.
17. Patnaik SK, Stanley P. Lectin-resistant CHO glycosylation mutants. *Methods Enzymol*. 2006;416:159–182.
18. Limberis MP, Vandenberghe LH, Zhang L, Pickles RJ, Wilson JM. Transduction efficiencies of novel AAV vectors in mouse airway epithelium in vivo and human ciliated airway epithelium in vitro. *Mol Ther*. 2009;17(2):294–301.
19. Inagaki K, et al. Robust systemic transduction with AAV9 vectors in mice: efficient global cardiac gene transfer superior to that of AAV8. *Mol Ther*. 2006; 14(1):45–53.
20. Vandendriessche T, et al. Efficacy and safety of adeno-associated viral vectors based on serotype 8 and 9 vs. lentiviral vectors for hemophilia B gene therapy. *J Thromb Haemost*. 2007;5(1):16–24.
21. Cearley CN, Wolfe JH. Transduction characteristics of adeno-associated virus vectors expressing cap serotypes 7, 8, 9, and Rh10 in the mouse brain. *Mol Ther*. 2006;13(3):528–537.
22. Zakhour M, et al. The alphaGal epitope of the histo-blood group antigen family is a ligand for bovine norovirus Newbury2 expected to prevent cross-species transmission. *PLoS Pathog*. 2009;5(7):e1000504.
23. Marth JD. O-Glycans. In: Varki A, Cummings R, Esko J, Freeze H, Hart G, Marth J, eds. *Essentials of Glycobiology*. Cold Spring Harbor, New York, USA: Cold Spring Harbor Laboratory Press; 1999:101–113.
24. Bergelson JM, et al. Isolation of a common receptor for Coxsackie B viruses and adenoviruses 2 and 5. *Science*. 1997;275(5304):1320–1323.
25. Tomko RP, Xu R, Philipson L. HCAR and MCAR: the human and mouse cellular receptors for subgroup C adenoviruses and group B coxsackieviruses. *Proc Natl Acad Sci U S A*. 1997;94(7):3352–3356.
26. Alemany R, Curiel DT. CAR-binding ablation does not change biodistribution and toxicity of adenoviral vectors. *Gene Ther*. 2001;8(17):1347–1353.
27. Smith T, et al. In vivo hepatic adenoviral gene delivery occurs independently of the coxsackievirus-adenovirus receptor. *Mol Ther*. 2002;5(6):770–779.
28. Martin K, Brie A, Saulnier P, Perricaudet M, Yeh P, Vigne E. Simultaneous CAR- and alpha V integrin-binding ablation fails to reduce Ad5 liver tropism. *Mol Ther*. 2003;8(3):485–494.
29. Parker AL, et al. Multiple vitamin K-dependent coagulation zymogens promote adenovirus-mediated gene delivery to hepatocytes. *Blood*. 2006; 108(8):2554–2561.
30. Shayakhmetov DM, Gaggar A, Ni S, Li ZY, Lieber A. Adenovirus binding to blood factors results in liver cell infection and hepatotoxicity. *J Virol*. 2005; 79(12):7478–7491.
31. Waddington SN, et al. Targeting of adenovirus serotype 5 (Ad5) and 5/47 pseudotyped vectors in vivo: fundamental involvement of coagulation factors and redundancy of CAR binding by Ad5. *J Virol*. 2007;81(17):9568–9571.
32. Wisse E, Jacobs F, Topal B, Frederik P, De Geest B. The size of endothelial fenestrae in human liver sinusoids: implications for hepatocyte-directed gene transfer. *Gene Ther*. 2008;15(17):1193–1199.
33. Shen S, Bryant KD, Brown SM, Randell SH, Asokan A. Terminal N-linked galactose is the primary receptor for adeno-associated virus 9 [published online ahead of print March 2, 2011]. *J Biol Chem*. doi:10.1074/jbc.M110.210922 jbc.M110.210922.
34. Kohlbrenner E, et al. Successful production of pseudotyped rAAV vectors using a modified baculovirus expression system. *Mol Ther*. 2005;12(6):1217–1225.
35. Ng R, et al. Structural characterization of the dual glycan binding adeno-associated virus serotype 6. *J Virol*. 2010;84(24):12945–12957.
36. Mitchell M, et al. Production, purification and preliminary X-ray crystallographic studies of adeno-associated virus serotype 9. *Acta Crystallogr Sect F Struct Biol Cryst Commun*. 2009;65(pt 7):715–718.
37. Blixt O, et al. Printed covalent glycan array for ligand profiling of diverse glycan binding proteins. *Proc Natl Acad Sci U S A*. 2004;101(49):17033–17038.
38. Bell P, et al. An optimized protocol for detection of *E. coli* beta-galactosidase in lung tissue following gene transfer. *Histochem Cell Biol*. 2005;124(1):77–85.